Elsevier Editorial System(tm) for Water Research

Manuscript Draft

Manuscript Number: WR46191R1

Title: Tertiary treatment of urban wastewater by solar and UV-C driven advanced oxidation with peracetic acid: effect on contaminants of emerging concern and antibiotic resistance

Article Type: Research Paper

Keywords: advanced oxidation processes; antibiotic resistant bacteria; peracetic acid; solar driven processes; wastewater treatment; water disinfection

Corresponding Author: Professor Luigi Rizzo, PhD

Corresponding Author's Institution: University of Salerno

First Author: Luigi Rizzo, PhD

Order of Authors: Luigi Rizzo, PhD; Teresa Agovino; Samira Nahim Granados; Maria Castro-Alférez; Pilar Fernández-Ibáñez; Maria I Polo-López

Abstract: Photo-driven advanced oxidation process (AOP) with peracetic acid (PAA) has been poorly investigated in water and wastewater treatment so far. In the present work its possible use as tertiary treatment of urban wastewater to effectively minimize the release into the environment of contaminants of emerging concern (CECs) and antibiotic-resistant bacteria was investigated. Different initial PAA concentrations, two light sources (sunlight and UV-C) and two different water matrices (groundwater (GW) and wastewater (WW)) were studied. Low PAA doses were found to be effective in the inactivation of antibiotic resistant Escherichia coli (AR E. coli) in GW, with the UV-C process being faster (limit of detection (LOD) achieved for a cumulative energy (QUV) of 0.3 kJL-1 with 0.2 mg PAA L-1) than solar driven one (LOD achieved at QUV=4.4 kJL-1 with 0.2 mg PAA L-1). Really fast inactivation rates of indigenous AR E. coli were also observed in WW. Higher QUV and PAA initial doses were necessary to effectively remove the three target CECs (carbamazepine (CBZ), diclofenac and sulfamethoxazole), with CBZ being the more refractory one. In conclusion, photo-driven AOP with PAA can be effectively used as tertiary treatment of urban wastewater but initial PAA dose should be optimized to find the best compromise between target bacteria inactivation and CECs removal as well as to prevent scavenging effect of PAA on hydroxyl radicals because of high PAA concentration.

Reviewer #3 (R3): The article is not innovative. It is already known that the AOP with peracetic acid has good efficiency on disinfection, in fact, recently it was reported that UVC-PAA can be use for food sanitation. Due to this reason I don't think that it can to be publish in Water Research.

A: actually, the authors did not state that the novelty of their work was in the investigation of AOP with PAA for water disinfection. Moreover, the authors trust that the following sentences can better explain and summarize the novelty of their work:

1. The evaluation of the effect of UV/PAA process on the removal of contaminants of emerging concern (CECs) from water and wastewater at quite realistic concentrations (to authors' knowledge only one work investigated this issue so far);
2. The evaluation of the effect of **solar** driven AOP with PAA on the removal of CECs from water and wastewater at quite realistic concentrations (to authors' knowledge no work that investigated this issue is available in scientific literature);
3. The effect of PAA based AOP on antibiotic resistance (in terms of antibiotic resistant bacteria (ARB) inactivation) (to authors' knowledge no work that investigated this issue is available in scientific literature);
4. The effect of PAA based AOP on the simultaneous removal of CECs and ARB in real water matrices to evaluate how the process should be operated under real conditions (to authors' knowledge no work that investigated this issue is available in scientific literature).

Highlights

- First time sunlight/PAA investigated in the removal of CECs
- Low PAA doses effective in the inactivation of AR *E. coli* by UV-C/PAA and sunlight/PAA
- Higher Q_{UV} and PAA initial doses are necessary to effectively remove the target CECs
- UV-C/PAA faster than sunlight/PAA in AR *E. coli* inactivation and CECs removal
- Sunlight/PAA possible option for tertiary treatment in small wastewater treatment plants

Graphical Abstract

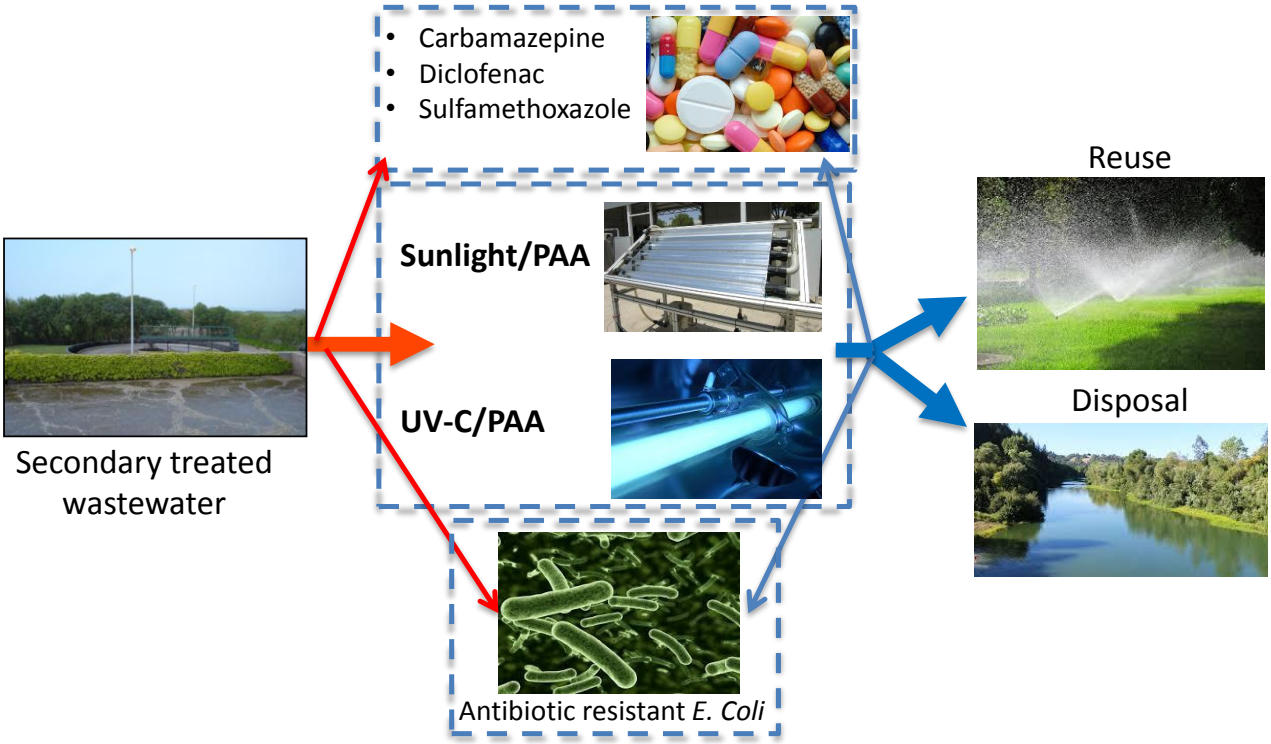

Tertiary treatment of urban wastewater by solar and UV-C driven advanced oxidation with peracetic acid: effect on contaminants of emerging concern and antibiotic resistance

Luigi Rizzo[1,*], Teresa Agovino[1], Samira Nahim-Granados [2], María Castro-Alférez [2], Pilar Fernández-Ibáñez [3], María Inmaculada Polo-López[2,*]

[1]Department of Civil Engineering, University of Salerno, Via Giovanni Paolo II 132, 84084 Fisciano (SA), Italy

[2] CIEMAT-Plataforma Solar de Almeria, P.O. Box 22, Tabernas (Almería), Spain.

[3]Nanotechnology and Integrated BioEngineering Centre, School of Engineering, University of Ulster, Newtownabbey, Northern Ireland, United Kingdom

*Corresponding authors: l.rizzo@unisa.it, mpolo@psa.es

Abstract

Photo-driven advanced oxidation process (AOP) with peracetic acid (PAA) has been poorly investigated in water and wastewater treatment so far. In the present work its possible use as tertiary treatment of urban wastewater to effectively minimize the release into the environment of contaminants of emerging concern (CECs) and antibiotic-resistant bacteria was investigated. Different initial PAA concentrations, two light sources (sunlight and UV-C) and two different water matrices (groundwater (GW) and wastewater (WW)) were studied. Low PAA doses were found to be effective in the inactivation of antibiotic resistant *Escherichia coli* (AR *E. coli*) in GW, with the UV-C process being faster (limit of detection (LOD) achieved for a cumulative energy (Q_{UV}) of 0.3 kJL^{-1} with 0.2 mg PAA L^{-1}) than solar driven one (LOD achieved at Q_{UV}=4.4 kJL^{-1} with 0.2 mg PAA L^{-1}). Really fast inactivation rates of indigenous AR *E. coli* were also observed in WW. Higher Q_{UV} and PAA initial doses were necessary to effectively remove the three target CECs (carbamazepine (CBZ), diclofenac and sulfamethoxazole), with CBZ being the more refractory one. In conclusion, photo-driven AOP with PAA can be effectively used as tertiary treatment of urban wastewater but initial PAA dose should be optimized to find the best compromise between target bacteria inactivation and CECs removal as well as to prevent scavenging effect of PAA on hydroxyl radicals because of high PAA concentration.

Keywords: advanced oxidation processes, antibiotic-resistant bacteria, peracetic acid, solar driven processes, wastewater treatment, water disinfection.

1. Introduction

The concern for the release into the environment of micro-contaminants from point sources, such as wastewater treatment plants (Petrie et al., 2015), as well as the need of wastewater reuse, due to the lack of fresh water sources (Fatta Kassinos, 2015), have been stimulating the discussion in the last years about new relevant regulations (JRC, 2015; Brack et al., 2017) to make urban wastewater treatment plants (UWTPs) effluents safer. As matter of fact, because of inconsistent national legislation across Member States, the European Commission is working on a legislative proposal on minimum quality requirements (MQR) for water reuse in agricultural irrigation and aquifer recharge (Rizzo et al., 2018). Meanwhile, in the attempt to minimize the release of micro-contaminants (also known as contaminants of emerging concern, CECs) from UWTPs in the environment, Switzerland enacted a regulation entered into force on January 2016, which requires the upgrade of UWTPs within the next twenty years (www.bafu.admin.ch). Accordingly, a selection of CECs from a list of twelve compounds need to be removed from the effluent by 80% (Bourgin et al. 2018). The increasing interest toward CECs and other emerging contaminants, such as antibiotic-resistant bacteria (ARB) and genes (ARGs), as well as the ongoing discussion on new related regulations, have driven the attention on UWTPs that are not or poorly effective to successfully address these new challenges (Rizzo et al., 2013; Petrie et al., 2015; Krzeminski et al., 2019). In a multi-barrier approach, typically implemented in UWTPs trains, the most important role to minimize the release of CECs and the risk of antibiotic resistance spread into the environment relies on tertiary treatment (Ferro et al., 2015; Bourgin et al. 2018). Unfortunately, consolidated tertiary treatments either did not show to be effective or did result in some drawbacks. As matter of fact, chlorination, typically used as disinfection step before UWTP effluent disposal or reuse, is poorly effective in the removal of CECs (Fu et al., 2018) and in controlling antibiotic resistance (Fiorentino et al., 2015; Yuan et al.,

2015), as well as results in the formation of hazardous disinfection by-products (DBPs) (Huang et al., 2016; Keun-Young et al., 2016). UV-C disinfection is effective in the inactivation of pathogens when sand filtration is used as pre-treatment, but poor or not effective at all (depending on the characteristics of the target molecule) in the removal of CECs (Lian et al., 2015). Tertiary treatment by ozonation can inactivate pathogens and remove CECs, but an additional post-treatment step can be necessary to remove ozonation by-products (i.e., nitrosodimetylamine and bromate) (Hollender et al., 2009). Activated carbon adsorption is also an effective tertiary treatment for the removal of CECs (Rizzo et al., 2015; Ahmed, 2017) but an additional disinfection process may be necessary, in particular to meet more stringent standards for wastewater reuse. Due to their efficiency in the removal of CECs and inactivation of pathogens because of the formation of reactive oxygen species (ROS), such as hydroxyl radicals ($HO^{\bullet}$), advanced oxidation processes (AOPs) represent a possible alternative to conventional tertiary treatments. AOPs can be classified in different ways, one being photo (among which UV/H_2O_2, photo-Fenton and TiO_2 photocatalysis) and not photo (such as Fenton, O_3, O_3/H_2O_2 etc.) driven AOPs. Photo-driven AOPs, can be also operated with solar radiation to save energy costs (Malato et al., 2009). Homogeneous photo-driven AOPs (such as UV/H_2O_2 and photo-Fenton) are more attractive than heterogeneous photocatalytic processes (such as UV/TiO_2) for short term application as tertiary treatment method of urban wastewater. As matter of fact, the technology of heterogeneous processes is not yet fully mature for large scale applications, basically for limitations related either to catalyst removal after treatment or fixing catalyst on a support (Sacco et al., 2018), and it would be more expensive than homogeneous photo-driven AOPs based technology. Peracetic acid (PAA) is increasingly used as an alternative option to chlorination in wastewater disinfection (Antonelli et al., 2013; Formisano et al., 2016). However, disinfection efficiency (Formisano et al., 2016) and CECs removal (Cai et al., 2017) may be improved by coupling PAA with UV radiation,

due to the formation of $HO^{\bullet}$. Accordingly, the possible use of this process as homogeneous photo-driven AOP for tertiary treatment of urban wastewater is worthy of investigation. In particular, before any possible up-scale it would be of interest to examine the process efficiency in the removal of CECs at environmentally significant concentrations as well as its effect on antibiotic resistance. Therefore, in the present work, UV/PAA process at pilot scale was investigated for the first time in the inactivation of an antibiotic resistant (AR) (sulfamethoxazole) *Escherichia coli* (*E. coli*) strain, and in the degradation of a mixture of three CECs: (anticonvulsant) Carbamazepine (CBZ), (analgesic) Diclofenac (DCF) and (antibiotic) Sulfamethoxazole (SMX), at initial concentration of 100 μgL^{-1} each, in a lower complexity aqueous matrix (namely groundwater (GW)). Subsequently, UV/PAA process was investigated on secondary treated wastewater (WW) samples to evaluate the inactivation of indigenous AR *E. coli* and the degradation of the same mixture of CECs. The effect of light source (solar light Vs UV-C radiation) was also investigated in both aqueous matrices (GW and WW). *E. coli* was chosen as model microorganism because it is considered among the most important vectors in the dissemination of antimicrobial resistance in the environment (Rizzo et al., 2013) as well as because it is used as pathogen indicator in regulations and guide lines for wastewater disposal and reuse (USEPA, 2012; ISO, 2015). CBZ, DCF and SMX were selected as model CECs because they are typically detected in urban wastewater (Petrie et al., 2015).

2. Material and methods

2.1 Chemicals

Carbamazepine (CBZ), Diclofenac (DCF) and Sulfamethoxazole (SMX), all high purity grade (>99%), were purchased from Sigma-Aldrich. Peracetic Acid (PAA) solution, containing 30% w/w of PAA and 4.5 % w/w of H_2O_2 was purchased from Sigma-Aldrich

and used as obtained. Sodium thiosulfate ($Na_2S_2O_3$, 99% w/w) and bovin liver catalase were used, as received from Sigma-Aldrich. Titanium IV oxysulfate (Riedel-de-Haën, Germany) was used, as obtained from the manufacturer.

2.2 Water matrices

To evaluate water matrix effect on UV/PAA process tests were performed with both GW and WW. GW was collected from a borehole located on the PSA site with depth of approximately 200 m. Physical-chemical characteristics of both water matrices are given in Table 1.

Table 1

GW samples were inoculated with SMX resistant *E. coli* strain selected from the effluent of the biological process (activated sludge) of Almeria (Spain) UWTP, according to the procedure explained in the subsequent paragraph 2.4. WW samples were also taken after biological process (just upstream of disinfection unit) from the same UWTP during spring-summer time (June-August 2017), and used for disinfection/oxidation experiments without inoculum. Samples were collected in amber glass bottles and stored at 4 °C for a maximum of two days.

2.3 AOPs and control experiments

The experimental design included two pilot scale reactors, namely a Compound Parabolic Collector (CPC) for outdoor sunlight experiments and a UV-C reactor (UV-C).

138

139 2.3.1 Sunlight/PAA experiments with CPC

140 The CPC reactor used was previously described (Polo-López et al., 2010). Briefly, it
141 consists of two 60 L tube modules, each one equipped with 10 cylindrical glass tubes made
142 of borosilicate glass, with a diameter of 5 cm, a length of 150 cm and a thickness of 2.5
143 mm, to allow a 90% transmission of UVA in the natural solar spectrum. The photoreactor
144 is titled at 37° with respect to the horizontal to maximize solar radiation. A tank housed in
145 the lower part of the pilot plant is connected to a pump, which allowed to operate the
146 modules in a recirculation mode. The CPC reactor has a total illuminated volume of 45 L
147 and it was operated with a water flow rate of 30 $Lmin^{-1}$. This flow rate guarantees a
148 turbulent regime, which results in a proper homogenization of water samples and in a good
149 contact between bacteria, contaminants and oxidant. Disinfection experiments were carried
150 out during 300 minutes of solar exposure on clear sunny days at PSA from May 2017 to
151 August 2017. More specifically, firstly the solar photoreactor was filled in with 60 L of
152 water matrix (GW or RW) and then, the mixture of the three CECs (100 μgL^{-1} of initial
153 concentration each) and the sulfamethoxazole resistant *E.coli* solution (10^6 CFU mL^{-1}
154 initial bacterial density) were spiked in. After 5 minutes of homogenization with the CPC
155 still covered, a control sample was taken in order to ensure the presence of bacteria and
156 contaminants. Then, PAA (initial concentration in the range 0.075 – 20 mg L^{-1}) was added
157 to the reactor tank and after 10 minute of recirculation, the experiment started as the cover
158 was removed. Samples were collected at regular intervals depending on the treatment.
159 Water temperature ranged from 21.0 to 47.7 °C and pH ranged from 8.04 to 9.41. A fixed
160 pyranometer (Model CUV5, 280-400 nm, Kipp & Zonen, Netherlands) registered in
161 continuous mode the incident light. The inactivation and degradation rates were plotted as
162 a function of both the experimental time (t) and the cumulative energy per unit of volume

(Q_{UV}) received in the photoreactor, commonly used to compare results under different conditions (Malato et al., 2009), and calculated by Equation (1):

$$Q_{UV,n} = Q_{UV,n-1} + \Delta t_n \cdot UV_{G,n} \cdot A_r/V_t \qquad \Delta t_n = t_n - t_{n-1} \qquad \text{(Eq.1)}$$

where $Q_{UV,n}$ and $Q_{UV,n-1}$ is the UV energy accumulated per liter (kJ L^{-1}) at times n and n-1, $UV_{G,n}$ is the average incident radiation on the irradiated area, Δt_n is the experimental time of sample, A_r is the illuminated area of the reactor (m^2) and V_t is the total volume of water treated (L). Each experiment was performed in duplicate, between 10 am to 16 pm local time, and the results were plotted as the average of the two replicates.

2.3.2 UV-C plant

The UV-C reactor is a plant equipped with three UV-C lamps (254 nm peak wavelengths, 230 W) connected in series, with a flexible configuration that allow the system to operate with a single lamp, two or three lamps in recirculating batch mode or continuous flow mode. In this study, only one lamp was used and the illuminated volume was 4.17 L, which corresponds to a total volume in the plant of 80 L. Disinfection/oxidation experiments were carried out during 180 minutes at PSA from May 2017 to August 2017. More specifically, firstly the reactor was filled in with water matrix (GW or WW) and then, the mixture of the three CECs (100 $\mu g L^{-1}$) and the sulfamethoxazole resistant *E.coli* solution (10^6 $CFU mL^{-1}$) were spiked in. After 15 minute of homogenization, with the lamp still switched off, initial sample was taken in order to ensure the presence of bacteria and contaminants. Then, PAA (initial concentration in the range 0.075 – 20 mg L^{-1}) was added to the reactor tank and after 15 minute of recirculation, the experiment started and the lamp was switched on. Samples were collected at regular intervals depending on the treatment. A fixed controller (ProMinent) housed in the back of the reactor, monitored in continuous water flow rate (46

187 Lmin^{-1}) and UV-C lamp intensity (33.7 Wm^{-2} for WW and 99.7 Wm^{-2} for GW). The
188 equipment registers, in continuous during the test, the sensor measurements in terms of
189 incident irradiation (Wm^{-2}), which is the UV-C radiation energy rate incident on a surface
190 per unit area. The accumulated energy was calculated according to Eq. 2:

191 $Q_{UVC}\ (kJ\ L^{-1}) = \text{Dose}\ (Jm^{-2}) \cdot A_i / V_T (m^2 L^{-1})(kJ(1000\ J)^{-1})$ (Eq.2)

192 where Q_{UVC} is the accumulated UV-C energy per L, Dose is the UV-C ultraviolet
193 irradiation (Wm^{-2}) emitted by the lamp multiplied by the illumination time, A_i (0.28 m^2) is
194 the irradiated surface, V_T (80 L) is the total volume of the water into the pilot plant and Vi
195 (4.17 L) is the total irradiated volume. Each experiment was performed in duplicate and the
196 results were plotted as the average of the two replicates.

197

198 2.4 Selection of antibiotic resistant *E. coli* strain

199 The antibiotic resistant *E.coli* strain inoculated in GW for disinfection experiments was
200 isolated from the effluent of the biological process (activated sludge) of Almeria UWTP by
201 membrane filtration method and subsequent cultivation on selective medium, according to
202 a previously published procedure (Rizzo et al., 2014). More specifically, 50 mL of
203 wastewater and its serial dilutions were filtered through sterile membranes (cellulose
204 nitrate, 0.45-µm pore size, 47 mm diameter, Millipore) which were incubated (24 h, 37 °C)
205 on AR m-FC (Difco) culture medium supplemented with 64 mgL^{-1} of sulfamethoxazole.
206 Antibiotic concentration was chosen according to the double of the respective minimum
207 inhibitory concentration (MIC) values available in EUCAST database (2014). Some
208 colonies were randomly picked up and frozen at -5 °C using sterile vials of cryobeads
209 (Deltalab). To recover the stock, the vial was slowly unfreezed up to reach room
210 temperature (25 ºC). One bead was streaked onto a Petri dish of AR m-FC agar and

incubated for 20 h at 37 ºC to obtain isolated bacteria colonies. This dish was stored during 1 week in the refrigerator to prepare a fresh *E. coli* culture to make it available for GW disinfection/oxidation experiments. Fresh liquid cultures were prepared taking one colony from the refrigerated stock in the Petri dish using a loop, transferred into 14 mL of liquid LB broth and incubated in a rotary shaker at 100 rpm, during 18-20 h at 37 ºC to get the bacterial stationary phase concentration (10^9 CFU mL^{-1}). Bacterial suspensions were harvested by centrifugation at 3000 rpm for 10 min. Then, the pellet was re-suspended in Phosphate Buffer Saline (PBS) solution and diluted directly into the GW sample for each experiment to reach the initial concentration of 10^6 $CFUmL^{-1}$.

2.5 Analytical measurements

Before performing each experiment, water samples were characterized in terms of temperature, pH, conductivity, DOC, inorganic carbon (IC), total carbon (TC), anions and cations. Temperature and pH were measured using a multi parametric sensor WTW multi720. Conductivity was measured by a conductivity meter GLP31 CRISON. Turbidity was measured by a turbidity meter 2100AN model (Hach). DOC, IC and TC were analyzed using a Shimadzu TOC-V-CSN and an auto-sampler ASI-V. DOC was estimated as the difference between the TC and the IC values. Samples were filtered with a 0.22 mm nylon filter (Aisimo, Millipore Millex® GN) before their injection into the equipment. The calibration was performed periodically with potassium hydrogen phthalate in Milli-Q water for TC and a sodium carbonate/sodium bicarbonate (1:1) for IC. Anions and cations were analyzed using ion chromatography, 850 Professional IC – Cation coupled to Metrohm 872 Extension Module. Samples were filtered with a 0.22 mm nylon filter (Aisimo) before injection into the equipment. The calibration was checked before samples measurements by standard solutions of 10 mg L^{-1} of each anion and cation analyzed. CECs concentrations

were monitored by ultra-performance liquid chromatography UPLC (Agilent Technologies, series 1200) with a UV-DAD detector and a C-18 analytical column. The initial conditions were 95% water with 25 mM formic acid (A) and 5% ACN (B). A linear gradient progressed from 10% to 0% B in 15 min. Re-equilibration time was 3 min with a flow rate of 1 $mL \cdot min^{-1}$. In order to prepare the vial for the detector, firstly, 4.5 mL of sample were filtered using a 0.22-μm PTFE filter (Millipore). Then, to remove any adsorbed compounds, the filter was washed with 2.5 mL of ACN mixed with the filtered water sample. The prepared solution was transferred into an amber glass vial, put in the UPLC and analyzed using an injection volume of 100 μL. Retention time, quantification limit (LOQ), detection limits (LOD) and maximum absorption (l) for the MCs are shown in Table S1 (in supplementary information file).

PAA commercially available solutions also contain a percentage of H_2O_2 (4.5 % w/w in the solution used in this work), which will contribute to the formation of $HO^{\bullet}$. Accordingly, H_2O_2 residual concentration was also measured in this work to better support explanation and discussion of the results achieved. In particular, H_2O_2 concentration was measured with a spectrophotometer (PG Instruments Ltd T-60-U) at 410 nm in glass cuvettes with a 1 cm of path length based on the formation of a yellow complex from the reaction of titanium IV oxysulfate with H_2O_2 following DIN 38409 H15. Absorbance was read after 5 min incubation time against a H_2O_2 standard curve linear in the 0.1 - 100 mgL^{-1} concentration range.

PAA concentration was measured according to the method from HACH (2014). Briefly, 2.5 ml of sample was mixed with 15 mg of N,N-diethyl-p-phenylenediamine (DPD, VWR Chemicals). Absorbance was measured with a spectrophotometer (PG Instruments Ltd T-60-U) at 530 nm after 45 seconds of incubation time against a PAA standard curve (range 0.05 – 5 mg L^{-1}).

261

262 2.6 Bacterial count

263 Bacterial count was performed by standard plate counting method through a serial 10-fold
264 dilutions in PBS placed into AR m-FC agar Petri dishes. In particular, when the bacterial
265 load was expected to be high, 50 μL drop of adequate dilution was plated, instead, when
266 the bacterial load was expected to be low, volume of 500 μL was spread onto prepared
267 dishes. Antibiotic resistant (AR) *E.coli* colonies were counted after an incubation period of
268 20 h at 37 ºC (limit of detection (LOD) 2 $CFUmL^{-1}$). Measurements were carried out in
269 duplicates in order to plot average values. The results were highly reproducible and the
270 standard deviation of the replicates is showed in the graphs as error bars. Stock solutions of
271 bovine liver catalase (50 mg L^{-1}) and sodium thiosulfate (100 mg L^{-1}) were freshly
272 prepared every day and added 20 μL mL^{-1} and 1 μL mL^{-1} respectively to all water samples
273 taken from the reactors in order to remove any residual concentration of PAA and H_2O_2.

274

275 **3. Results**

276 *3.1 Inactivation of AR E. coli by sunlight/PAA in CPC*

277 3.1.1 Control tests

278 Control experiments were performed with PAA and sunlight as standalone processes,
279 respectively. The effect of PAA on the inactivation of AR *E. coli* under dark conditions
280 was investigated for three PAA concentrations (0.075, 1 and 2 mg L^{-1}) in GW. The LOD
281 was achieved for 1 and 2 mg PAA L^{-1}, with 4 and 5 log unit inactivation respectively, after
282 15 min (Figure 1). The lower investigated dose (0.075 mg PAA L^{-1}) resulted only in half
283 log unit inactivation after 180 min, possibly due to the low initial concentration of both

PAA and H_2O_2 (0.039 mg L^{-1}). The LOD was even achieved for sunlight experiment, but after 300 minutes treatment (53.67 kJL^{-1}).

Figure 1

Part of PAA initial concentration was consumed as the oxidant solution was added to GW sample; as can be observed from Figure SI1, PAA concentration measured just after the addition of PAA solution (t=0) is lower than the corresponding initial concentration dosed. Moreover, PAA was almost totally consumed after 300 min treatment when 1 mg PAA L^{-1} was added; while only 50% was consumed when initial PAA was 2 mg PAA L^{-1}.

3.1.2 Effect of PAA initial concentration

Since AR *E. coli* inactivation was quite fast between 1 and 2 mg PAA L^{-1} under dark conditions, lower PAA concentrations (in the range 0.075-1.0 mg L^{-1}) were investigated during sunlight/PAA tests. Q_{UV} and solar exposure time required to reach the LOD for the inactivation of AR *E.coli*, decreased as PAA dose was increased. More specifically, in GW the best performance was achieved after 30 minutes with 0.2 mg PAA L^{-1} (Q_{UV} = 4.40 kJL^{-1}) (Figure 2a). Inactivation rates were faster compared to sunlight experiment where LOD was achieved after 300 minutes treatment with a higher energy requirement (53.67 kJL^{-1}).

Figure 2

306 Moreover, the lower investigated PAA initial concentration (0.075 mg L^{-1}) did not produce
307 a sufficient amount of hydroxyl radicals to improve AR *E.coli* inactivation compared to
308 solar radiation as standalone process. PAA was almost totally consumed during treatment
309 process (Figure SI2a) and a fluctuation in residual H_2O_2 concentration (1 mg PAA L^{-1}
310 solution) was observed (Figure SI2b).

311 The effect of sunlight/PAA process was also investigated in WW (Figure 2b). WW was not
312 inoculated with the selected AR *E. coli* strain, therefore the inactivation curves refer to the
313 indigenous *E. coli* population resistant to SMX (initial bacterial density 70-7000 CFU mL^{-1}
314). In particular, different initial PAA concentrations (1, 2, 4 and 10 mg L^{-1}) were
315 investigated and the best performance was observed for 10 mg PAA L^{-1} being the LOD
316 achieved after 2 minutes irradiation (Q_{UV}= 0.28 kJL^{-1}) (Figure 2b). The LOD was
317 achieved for all the investigated conditions, being the sunlight process the slower (Q_{UV}=
318 38.03 kJ L^{-1} after 210 min). In agreement with the results observed in GW experiments,
319 PAA was almost totally consumed during treatment process in WW, for PAA initial
320 concentrations in the range 1–10 mg L^{-1}, and only when a higher dose (20 mg L^{-1}) was
321 investigated (to evaluate possible effect on CECs degradation) a residual was detected
322 (Figure SI3a). Fluctuation in residual H_2O_2 concentration (1 mg PAA L^{-1} solution) was
323 also observed in WW experiments (Figure SI3b).

324

325 *3.2 Degradation of CECs by sunlight/PAA in CPC*

326 Typically, when AOPs are investigated in the removal of pollutants from water, an effect
327 of water matrix composition can be observed, with a decreased process efficiency as the
328 complexity of the aqueous matrix increases (e.g., from deionized water solutions to GW
329 and WW). The decreased efficiency can be typically explained by the occurrence of readily

oxidized molecules (also known as oxidant demand of the target water matrix) in more complex water matrices compared to less complex ones. Actually, this behaviour was not evident in the removal of CBZ and DCF by sunlight/PAA, while it was evident for SMX, as explained in the subsequent paragraphs.

3.2.1 Control tests

Control experiments to evaluate the effect of PAA and sunlight as standalone processes, on the target CECs were also carried out. In particular, the effect of PAA dose in darkness was investigated at 2 mg L^{-1} initial concentrations (Figure 3).

Figure 3

Unlike of CBZ, DCF was effectively oxidized by PAA after 60 minutes (80% removal), while SMX was removed at a lower rate (52% after 300 min) compared to DCF. Photodegradation rate by sunlight as standalone process changed depending on the target CEC: from no degradation for CBZ, to moderate degradation for SMX (43% after 300 min irradiation and 53.7 kJ L^{-1}), to high degradation for DCF (90% after 180 min and 30.2 kJ L^{-1}).

3.2.2 Effect of PAA initial concentration

The effect of sunlight/PAA process on CECs was investigated for both water matrices (GW and WW). CBZ was refractory to sunlight/PAA process too. Only when initial PAA

352 concentration was increased to 10 mg L^{-1} a significant degradation (40%) was observed
353 after 300 min treatment (Q_{UV} = 55.53 kJ L^{-1}) in GW (Figure 4a).

354

355 **Figure 4**

356

357 Even for DCF, sunlight/PAA process enhanced degradation compared to PAA as
358 standalone process in GW matrix. The best performance was observed with 2 mg PAA L^{-1}
359 that allowed to reach the quantification limit (QL) at Q_{UV} =10.23 kJ L^{-1} (Figure 4b).
360 Interestingly, as PAA concentration was further increased from 4 to 10 mg L^{-1}, DCF
361 degradation rate decreased. Similar behaviour was observed for SMX (Figure 4c). SMX
362 degradation increased as PAA dose was increased from the lower dose (0.075 mg L^{-1}) to 4
363 mg L^{-1} (the QL was reached after 60 min and Q_{UV}= 9.49 kJ L^{-1}) then started to decrease,
364 although to a lower rate compared to DCF.

365 Due to the higher oxidant demand of WW, PAA doses lower than 1.0 mg L^{-1} were not
366 investigated and 20 mg PAA L^{-1} was added (Figure 5). The behaviour of sunlight/PAA
367 process in WW matrix was quite different compared to GW. As matter of fact, a moderate
368 efficiency in CBZ degradation was also observed at lower PAA doses; for example 2 mg
369 PAA L^{-1} resulted in 23% CBZ degradation after 300 min (Q_{UV} = 58.39 kJ L^{-1}) and process
370 efficiency increased as initial PAA concentration was increased to 4 and 10 mg L^{-1}, being
371 the best removal (56%) observed with 10 mg PAA L^{-1} after 300 minutes (Q_{UV}= 58.39 kJ L^{-1})
372) (Figure 5a). But as PAA was further increased (20 mg L^{-1}), process efficiency drastically
373 decreased, thus showing a similar behaviour to DCF and SMX in GW experiments.

374

Figure 5

DCF degradation was drastically affected by aqueous matrix. The best performance in WW was observed with 20 mg PAA L^{-1} that reached the QL after 120 min (Q_{UV} = 11.46 kJ L^{-1}) (Figure 5b). Moreover, aqueous matrix significantly affected process efficiency at lower PAA concentrations; for example, only 32% degradation was achieved with 2 mgL^{-1} of PAA in WW, compared to 99% observed in GW after 60 min treatment (Q_{UV} = 10.23 kJ L^{-1}). Similarly to the results observed for GW, SMX degradation by sunlight/PAA increased as PAA concentration was increased (Figure 5c). The QL was achieved for 10 mg L^{-1} of PAA after 240 min (Q_{UV}= 46.03 kJ L^{-1}). But a further increase of initial PAA dose to 20 mg L^{-1} resulted in a decreased degradation efficiency, thus confirming the trend already observed in GW experiments.

3.3 Inactivation of AR E. coli by UV-C/PAA process

Really fast inactivation rates were observed in GW for UV-C/PAA process compared to sunlight/PAA (Figure 6). The LOD was achieved for all PAA investigated doses and even for UV-C as standalone process. In particular, total inactivation was achieved in a few minutes for 0.15 mg PAA L^{-1} (2 min) and 0.2 mg PAA L^{-1} (4 min).

Figure 6

With 0.075 mg L^{-1} and 0.1 mgL^{-1} of PAA LOD was reached with a cumulative energy dose of 67.39 kJL^{-1} (180 min irradiation) and 33.93 kJL^{-1} (90 min irradiation), respectively.

Due to both the higher oxidant demand of WW compared to GW and the total consumption of PAA and H_2O_2 in GW experiments, higher concentrations of PAA (4, 10 and 20 mgL^{-1}) were investigated in UV-C/PAA experiments in WW. As matter of fact, the initial AR *E. coli* concentrations were really low (63, 35 and 2 CFU mL^{-1} for 4, 10 and 20 mg PAA L^{-1} experiments, respectively) and the LOD was achieved in 2 and 15 min for 10 and 4 mg PAA L^{-1} experiments, respectively (data not shown).

3.4 Degradation of CECs by UV-C/PAA process

The effect of PAA dose on the degradation of the target CECs by UV-C/PAA process was investigated in both water matrices (GW and WW). Among the three CECs, CBZ confirmed its lower degradation. No significant differences were observed between UV-C as standalone process (20% degradation after 180 minutes treatment and with an energy requirement of 71.78 kJ L^{-1}) and UV-C/PAA process up to 1.0 mg PAA L^{-1} in GW (Figure 7a). The best performance (77% removal) was obtained with 10 mg PAA L^{-1} after 150 minutes and with a Q_{UVC} of 71.78 kJ L^{-1}. Residual concentrations of PAA and H_2O_2 are available in supplementary information (Figures SI4a and SI4b).

Figure 7

For the lower concentration investigated in WW (4 mg PAA L^{-1}) the aqueous matrix effect between GW and WW was not observed (Figure 7b). But when PAA concentration was increased (10 and 20 mg PAA L^{-1}) the difference between the two matrices increased (e.g., 55% CBZ removal in WW compared to 67% in GW for 10 mg PAA L^{-1} at approximately

21 kJ L^{-1}). Interestingly, at the higher investigated dose (20 mg PAA L^{-1}), the residual concentration of PAA is lower than that one for 10 mg PAA L^{-1} solution, but the corresponding H_2O_2 residual concentration is significantly higher (Figure SI5).

The best degradation of DCF in GW was observed for the lower investigated PAA doses (0.075 mg PAA L^{-1}) compared to sunlight/PAA tests (Figure 8a). Even in UV-C/PAA tests, process efficiency started to decrease above a certain concentration (1.0 mg L^{-1}) of PAA, being the worst removal observed for the higher investigated PAA dose (10 mg L^{-1}). The water matrix affected the photo-oxidation process, because no drastic efficiency decrease was observed as PAA was increased (Figure 8b).

Figure 8

SMX was effectively degraded even with UV-C as stand-alone process in GW (LOD was achieved with Q_{UV}= 5.78 kJ L^{-1}) and WW (LOD observed for $Q_{UV<}$ 4.58 kJ L^{-1}), accordingly PAA addition did not significantly improve process efficiency (for 4 mg PAA L^{-1} LOD observed for $Q_{UV<}$ 2.4 kJ L^{-1}) (data not shown).

4. Discussion

4.1 Photolysis of PAA and effect on PAA and H_2O_2 concentrations

UV/PAA process has been poorly investigated so far, and the previous works have been basically focused on bacteria inactivation (Koivunen and Heinonen-Tanski, 2005; de Souza et al. 2015); only recently its effect on pharmaceuticals has been addressed (Cai et

al., 2017). PAA (CH_3CO_3H) aqueous solutions commercially available are an equilibrium mixture of acetic acid (CH_3COOH), H_2O_2, PAA and water, according to the reaction:

$$CH_3COOH + H_2O_2 \leftrightarrow CH_3CO_3H + H_2O \quad \text{(Eq.3)}$$

Photolysis of the O–O bond in the PAA molecule results in the formation of $HO^{\bullet}$, according to Equation 4 (Caretti and Lubello, 2003):

$$CH_3CO_3H + hv \rightarrow CH_3COO^{\bullet} + HO^{\bullet} \quad \text{(Eq.4)}$$

The $CH_3COO^{\bullet}$ molecule will rapidly split in $CH_3^{\bullet}$ and CO_2 (Martin and Gehr, 2007). Moreover, $HO^{\bullet}$ molecules can also recombine to form H_2O_2:

$$HO^{\bullet} + HO^{\bullet} \rightarrow H_2O_2 \quad \text{(Eq.5)}$$

The production of PAA (Eq.3) and the recombination of $HO^{\bullet}$ molecules (Eq.5) can explain the fluctuations observed in the measurement of residual H_2O_2 (Figure SI2b and SI3b).

According to the results achieved in this work, the mechanisms of bacterial inactivation and CECs degradation in PAA photolysis are possible related to a combination of effects including photolysis, oxidation (by PAA solution) and formation of $HO^{\bullet}$.

4.2 Control tests: effect of radiation and PAA solution on bacteria inactivation and CECs degradation

The effect of sunlight and UV-C radiation on bacteria inactivation is evident from figures 2 and 6, respectively. To date, all waterborne pathogenic bacteria, among which *E. coli*, have been found to be amenable to sunlight disinfection (McGuigan et al., 2012). Although the UV-A wavelengths are not sufficiently energetic to alter DNA directly, UV-A play an important role in promoting the formation of intracellular reactive oxygen species (e.g.,

465 $HO^{\bullet}$) which can, in turn, damage DNA. UV-C radiation (200–280 nm germicidal
466 wavelength range, peaks at about 260–265 nm) has a direct effect on bacterial cells
467 because it is absorbed by nucleic acids; cell inactivation can take place through UV-
468 induced damages such as the formation of pyrimidine dimers in their DNA (Kowalski,
469 2009).

470 While CBZ was not (under sunlight in GW) or poorly (under sunlight in WW and under
471 UV-C radiation) photodegraded, confirming its refractory behaviour to direct photolysis
472 (Calisto et al., 2011), SMX and DCF were significantly degraded under irradiation. DCF
473 has an absorbance peak at 275-280 nm and its degradation under sunlight is the result of
474 two mechanisms: direct photolysis and self-sensitization, being direct photolysis the main
475 one (Zhang et al., 2011). SMX absorbance spectrum is characterized by a peak at 257-268
476 nm (depending on solution pH) and tails well over 320 nm, which overlap with the solar
477 spectrum (in the 300–325 nm) and make its photodegradation possible (Trovò et al., 2009;
478 Rizzo et al., 2012).

479 The redox potential of PAA is comparable or even higher than many disinfectants (Zhang
480 et al., 2018), which make it effective in the inactivation of different bacterial populations.
481 Accordingly, our results in terms of AR *E. coli* inactivation under dark conditions (Figure
482 1) are consistent with previous results on *E. coli* inactivation (Antonelli et al., 2009).
483 Moreover, the high redox potential can also explain the high oxidation rate of DCF and
484 SMX (Figure 3).

485

4.3 *Effect of photo-driven AOPs with PAA on bacteria inactivation and CECs degradation*

According to Eq.4, sunlight/PAA and UV-C/PAA processes result in the formation of $HO^{\bullet}$ species. The role of $HO^{\bullet}$ in the inactivation of *E. coli* was previously explained through the support of disinfection photocatalytic experiments (Cho et al. 2004). In subsequent studies, a killing mechanism where $HO^{\bullet}$ progressively damages the cell surface structures leading to the release of intracellular material/molecules was proposed (Foster et al., 2011). Inactivation of microorganisms by photo-driven advanced oxidation with PAA has been mainly investigated by using artificial light while, to our knowledge, only one study was specifically focused on sunlight/PAA process (Formisano et al., 2016) and no previous study evaluated the effect on the inactivation of AR *E. coli*. Formisano et al. (2016) observed a total inactivation of *E. coli* by sunlight/PAA (8 mg PAA L^{-1}) process after 120 minutes treatment (Q_{UV}= 7.42 kJ L^{-1}) in WW, with an initial *E. coli* density as high as 10^5 CFU mL^{-1}. These results are different compared to the inactivation rates observed in our work with (i) GW (where the best performance was achieved after 30 minutes with 0.2 mg PAA L^{-1} and Q_{UV} = 4.40 kJ L^{-1}) (Figure 2a) and (ii) WW (being the best performance and LOD achieved for 10 mg PAA L^{-1} after 2 minutes irradiation and Q_{UV}= 0.28 kJ L^{-1}) (Figure 2b). The different water matrix and *E. coli* population (total Vs AR *E. coli*) in case (i) and the lower initial bacterial density and the different *E. coli* population in case (ii) may explain the different results observed. Inactivation rates in GW drastically increased when UV-C radiation was used (LOD achieved within 2 minutes for 0.15 mg PAA L^{-1} and 4 minutes with 0.2 mg PAA L^{-1}) instead of sunlight. In WW experiments, the initial AR *E. coli* concentration was really low and the LOD was achieved for all the PAA doses investigated. In a previous work on wastewater disinfection by UV-C/PAA process, *E. coli*

510 inactivation of 3.6 and 4.5 log units were observed for 2 and 4 mg L^{-1} of PAA, respectively
511 and an UV-C dose as high as UV dose of 120 mW·s cm^{-2} (Lubello et al., 2002).

512 As the effect of photo-driven AOPs with PAA on CECs degradation is of concern, it is
513 worthy to mention that scientific literature is lacking. However, our results are consistent
514 with removal trends of CBZ, DCF and SMX observed in solar driven AOPs (namely
515 photo-Fenton) (Klamerth et al., 2010; Ferro et al., 2015). In our work CBZ was found to be
516 refractory to sunlight/PAA process, according to the results available in the literature for
517 other solar driven AOPs. For example, only 36.9% degradation (same initial CBZ
518 concentration) was observed after 300 minute sunlight/H_2O_2 (20 mg L^{-1}) treatment
519 (Q_{UV}=19.3 kJ L^{-1}) in WW (Ferro et al., 2015). When UV-C radiation was used as light
520 source in UV-C/PAA process, an higher efficiency was observed (77% removal,
521 Q_{UV}=71,78 kJ L^{-1}), but the removal efficiency (22%) observed for 1 mg PAA L^{-1} is not
522 consistent with previous work (90% removal within 30 min, CBZ initial concentration 1
523 μM) (Cai et al., 2017). Unlike of CBZ, high removal efficiencies were observed for DCF
524 and SMX in sunlight/PAA experiments, with significantly improved removals in UV-
525 C/PAA tests. However, DCF degradation was drastically affected by aqueous matrix, with
526 a remarkable decreased efficiency in WW (Figure 5b) compared to GW (Figure 4b), in
527 particular at lower PAA concentrations. These results can be explained by the higher
528 oxidant demand of WW compared to GW (confirmed by the PAA and H_2O_2 consumption
529 for tests with low concentrations of PAA, Figures SI2 and SI3). Water matrix effect was
530 also observed for SMX degradation by sunlight/PAA and its removal is consistent with
531 previous works with other solar driven AOPs. As matter of fact, Karaolia et al. (2017)
532 observed complete removal of SMX (initial spiked concentration 100 μg L^{-1}) by solar
533 photo-Fenton in urban wastewater in a CPC reactor (50 mg H_2O_2 L^{-1} and 5 mg Fe^{2+} L^{-1},
534 119 min of normalized irradiation time ($t_{30W,n}$)).

Interestingly, similar removal trends were observed for DCF and SMX in sunlight/PAA experiments, in both water matrices investigated. The removal efficiency first increased as initial PAA was increased, then started to decrease. Possibly, the reduced efficiency may be due to the scavenging effect of PAA on $HO^{\bullet}$ because of the higher PAA concentration (Cai et al., 2017).

5. Conclusions

Photo-driven AOP with PAA was investigated as possible tertiary treatment method of urban wastewater by evaluating its efficiency in the inactivation of AR *E. coli* and degradation of a mixture of three CECs under different light sources. Low PAA doses were found to be effective in the inactivation of AR *E. coli*, being UV-C driven process faster (LOD achieved at Q_{UV}=0.3 kJ L^{-1} with 0.2 mg PAA L^{-1}) than solar driven one (LOD achieved at Q_{UV}=4.4 kJ L^{-1} with 0.2 mg PAA L^{-1}). Higher Q_{UV} and PAA initial doses are necessary to effectively remove the target CECs (being CBZ the more refractory) and, although process efficiency in sunlight tests is lower compared to UV-C radiation, sunlight driven process is still an interesting option for small wastewater treatment plants taking into account that CECs occur at low concentrations (typically in the range ng L^{-1} - fractions of µg L^{-1}). However, initial PAA dose should be optimized to find the best compromise between target bacteria inactivation and CECs removal as well as to prevent scavenging effect of PAA on $HO^{\bullet}$ because of high PAA concentration.

Acknowledgements

The authors wish to thank European Commission for supporting Teresa Agovino's visit at Plataforma Solar de Almeria in the context of ERASMUS programme.

559 **References**

560 Ahmed, M. J., 2017. Adsorption of quinolone, tetracycline, and penicillin antibiotics from
561 aqueous solution using activated carbons: Review. Environmental Toxicology and
562 Pharmacology 50, 1-10.

563 Antonelli, M., Rossi, S., Mezzanotte, V., Nurizzo, C. 2006. Secondary Effluent
564 Disinfection: PAA Long Term Efficiency. Environmental Science & Technology 40, 4771-
565 4775.

566 Antonelli, M., Turolla, A., Mezzanotte, V., Nurizzo, C. 2013. Peracetic acid for secondary
567 effluent disinfection: A comprehensive performance assessment. Water Science &
568 Technology 68 (12), 2638-2644.

569 Bourgin, M., Beck, B., Boehler, M., Borowska, E., Fleiner, J., Salhi, E., Teichler, R., von
570 Gunten, U., Siegrist, H., McArdell, C. S., 2018. Evaluation of a full-scale wastewater
571 treatment plant upgraded with ozonation and biological post-treatments: Abatement of
572 micropollutants, formation of transformation products and oxidation by-products. Water
573 Research 129, 486-498.

574 Brack, W., Dulio, V., Ågerstrand, M., Allan, I., Altenburger, R., Brinkmann, M., Bunke,
575 D., Burgess, R.M., Cousins, I., Escher, B.I., Hernández, F.J., Hewitt, L.M., Hilscherová,
576 K., Hollender, J., Hollert, H., Kase, R., Klauer, B., Lindim, C., López Herráez, D., Miège,
577 C., Munthe, J., O'Toole, S., Posthuma, L., Rüdel, H., Schäfer, R.B., Sengl, M., Smedes, F.,
578 van de Meent, D., van den Brink, P.J., van Gils, J., van Wezel, A.P., Vethaak, A.D.,
579 Vermeirssen, E., von der Ohe, P.C., Vrana, B. 2017. Towards the review of the European
580 Union Water Framework management of chemical contamination in European surface
581 water resources. Science of the Total Environment 576, 720–737.

582 Cai, M., Sun, P., Zhang, L., Huang, C.-H. 2017. UV/Peracetic Acid for Degradation of
583 Pharmaceuticals and Reactive Species Evaluation. Environmental Science & Technology
584 51, 14217-14224.

585 Calisto, V., Rosário Domingues, M., Erny, G.L., Esteves, V.I. 2011. Direct
586 photodegradation of carbamazepine followed by micellar electrokinetic chromatography
587 and mass spectrometry. Water Research 45, 1095-1104.

588 Caretti, C., Lubello, C. 2003. Wastewater disinfection with PAA and UV combined
589 treatment: a pilot plant study. Water Research 37, 2365-2371.

590 Cho, M., Chung, H., Choi, W., Yoon, J. 2004. Linear correlation between inactivation of
591 E. coli and OH radical concentration in TiO2 photocatalytic disinfection. Water Research
592 38, 1069-1077.

593 De Souza, J.B., Queiroz Valdez, F., Jeranoski, R.F., de Sousa Vidal, C.M., Soares
594 Cavallini, G. 2015. Water and Wastewater Disinfection with Peracetic Acid and UV
595 Radiation and Using Advanced Oxidative Process PAA/UV. International Journal of
596 Photoenergy, Article ID 860845, http://dx.doi.org/10.1155/2015/860845

597 Fatta-Kassinos, D., Manaia, C., Berendonk, T.U., Cytryn, E., Bayona, J., Chefetz, B.,
598 Slobodnik, J., Kreuzinger, N., Rizzo, L., Malato, S., Lundy, L., Ledin, A. COST Action
599 ES1403: New and Emerging challenges and opportunities in wastewater REUSe
600 (NEREUS). Environmental Science Pollution Research 22, 7183-7186.

601 Ferro, G., Polo-López, M.I., Martínez-Piernas, A.B., Fernández-Ibáñez, P., Agüera A.,
602 Rizzo L. 2015. Cross-Contamination of Residual Emerging Contaminants and Antibiotic
603 Resistant Bacteria in Lettuce Crops and Soil Irrigated with Wastewater Treated by
604 sunlight/H_2O_2. Environmental Science & Technology 49, 11096-11104.

605 Fiorentino, A., Ferro, G., Castro, A.M., Polo-López, M.I., Fernández-Ibañez, P., Rizzo, L.
606 2015. Inactivation and regrowth of multidrug resistant bacteria in urban wastewater after
607 disinfection by solar-driven and chlorination processes. Journal of Photochemistry and
608 Photobiology B: Biology 148, 43-50.

609 Formisano, F., Fiorentino, A., Rizzo, L., Carotenuto, M., Pucci, L., Giugni, M., Lofrano,
610 G. 2016. Inactivation of Escherichia coli and Enterococci in urban wastewater by
611 sunlight/PAA and sunlight/H2O2 processes. Process Safety and Environmental Protection
612 104, 178-184.

613 Foster, H.A., Ditta, I.B., Varghese, S., Steele, A. 2011. Photocatalytic disinfection using
614 titanium dioxide: spectrum and mechanism of antimicrobial activity. Applied
615 Microbiology Biotechnology 90, 1847-1868.

616 Fu, W., Li, B., Yan, J., Y, H., Liyuan, C., Li, X. 2018. New insights into the chlorination of
617 sulfonamide: Smiles-type rearrangement, desulfation, and product toxicity. Chemical
618 Engineering Journal 331, 785-793.

619 HACH, 2014. Determination of Peracetic Acid and Hydrogen Peroxide in Water.
620 Application Note.

621 Hollender, J., Zimmermann, S.G., Koepke, S., Krauss, M., Mcardell, C.S., Ort, C., Singer,
622 H., von Gunten, U., Hansruedi, S. 2009. Elimination of Organic Micropollutants in a
623 Municipal Wastewater Treatment Plant Upgraded with a Full-Scale Post-Ozonation
624 Followed by Sand Filtration. Environmental Science & Technology 43, 7862-7869.

625 Huang, H., Wu, Q.-Y., Tang, X., Jiang, R., Hu, H.-Y. 2016. Formation of haloacetonitriles
626 and haloacetamides and their precursors during chlorination of secondary effluents.
627 Chemosphere 144, 297-303.

628 ISO 16075 (2015). Guidelines for Treated Wastewater Use for Irrigation Projects.
629 International Organization for Standardization, Geneva, Switzerland.

630 JRC (Joint Research Centre), 2015. Development of the first Watch List under the
631 Environmental Quality Standards Directive: Directive 2008/105/EC, as amended by
632 Directive 2013/39/EU, in the field of water policy. Raquel N. Carvalho, Lidia Ceriani,
633 Alessio Ippolito and Teresa Lettieri. Report EUR 27142 EN.

634 Karaolia, P., Michael-Kordatou, I., Hapeshi, E., Alexander, J., Schwartz, T., Fatta-
635 Kassinos, D. 2017. Investigation of the potential of a Membrane BioReactor followed by
636 solar Fenton oxidation to remove antibiotic-related microcontaminants. Chemical
637 Engineering Journal 310, 491-502.

638 Keun-Young, P., Su-Young C., Seung-Hoon L., Ji-Hyang K., Ji-Hyeon S. 2016.
639 Comparison of formation of disinfection by-products by chlorination and ozonation of
640 wastewater effluents and their toxicity to Daphnia magna. Environmental Pollution 215,
641 314-321.

642 Klamerth, N., Rizzo, L., Malato, S., Maldonado, M.I., Agüera, A., Fernández-Alba, A.R.
643 2010. Degradation of fifteen emerging contaminants at μg L-1 initial concentrations by
644 mild solar photo-Fenton in MWTP effluents. Water Research 44, 545-554.

645 Koivunen, J., Heinonen-Tanski, H. 2005. Inactivation of enteric microorganisms with
646 chemical disinfectants, UV irradiation and combined chemical/UV treatments. Water
647 Research 39, 1519-1526.

648 Kowalski, W. 2009. Ultraviolet Germicidal Irradiation Handbook, DOI 10.1007/978-3-
649 642-01999-9_2, Springer-Verlag Berlin Heidelberg.

650 Krzeminski, P., Tomei, M.C., Karaolia, P., Langenhoff, A., Almeida, C.M.A., Felis, E.,
651 Gritten, F., Andersen, H.R., Fernandes T., Manaia, C.M., Rizzo, L., Fatta-Kassinos, D.
652 2019. Performance of secondary wastewater treatment methods for the removal of
653 contaminants of emerging concern implicated in crop uptake and antibiotic resistance
654 spread: A review. Science of the Total Environment 648, 1052-1081.

655 Lian, J., Qiang, Z., Li, M., Bolton, J.R., Qu, J. 2015. UV photolysis kinetics of
656 sulfonamides in aqueous solution based on optimized fluence quantification. Water
657 Research 75, 43-50.

658 Lubello, C., Caretti, C., Gori, R., 2002. Comparison between PAA/UV and H2O2/UV
659 disinfection for wastewater reuse. Water Science and Technology.: Water Supply 2(1),
660 205-212.

661 Malato, S., Fernandez-Ibanez, P., Maldonado, M.I., Blanco, J., Gernjak, W., 2009.
662 Decontamination and disinfection of water by solar photocatalysis: recent overview and
663 trends. Catalysis Today 147, 1–59.

664 Martin, N., Gehr, R., 2007. Reduction of Photoreactivation with the Combined
665 UV/Peracetic Acid Process or by Delayed Exposure to Visible Light. Water Environment
666 Research 79, 991-999.

667 McGuigan, K.G., Conroy, R.M., Mosler, H.-J., du Preez, M., Ubomba-Jaswa, E.,
668 Fernandez-Ibanez, P. 2012. Solar water disinfection (SODIS): a review from bench-top to
669 roof-top. Journal of Hazardous Materials 235-236, 29-46.

670 Petrie, B., Barden, R., Kasprzyk-Hordern B. 2015. A review on emerging contaminants in
671 wastewaters and the environment: Current knowledge, understudied areas and
672 recommendations for future monitoring. Water Research 72, 3-27.

673 Polo-López, M.I., Fernández-Ibáñez, P., García-Fernández, I., Oller, I., Salgado-Tránsito,
674 I., Sichel, C. 2010. Resistance of Fusarium sp spores to solar TiO_2 photocatalysis:
675 influence of spore type and water (scaling-up results). Journal of Chemical Technology
676 and Biotechnology 85, 1038–1048.

677 Rizzo, L., Della Sala, A., Fiorentino, A., Li Puma, G. 2014. Disinfection of urban
678 wastewater by solar driven and UV lamp – TiO2 photocatalysis: effect on a multi drug
679 resistant Escherichia coli strain, Water Research 53, 145-152.

680 Rizzo, L., Fiorentino, A., Anselmo, A. 2012. Effect of solar radiation on multidrug
681 resistant E. coli strains and antibiotic mixture photodegradation in wastewater polluted
682 stream. Science of the Total Environment 427-428, 263-268.

683 Rizzo, L., Fiorentino, A., Grassi, M, Attanasio, D., Guida M. 2015. Advanced treatment of
684 urban wastewater by sand filtration and graphene adsorption for wastewater reuse: Effect
685 on a mixture of pharmaceuticals and toxicity. Journal of Environmental Chemical
686 Engineering 3, 122-128.

687 Rizzo, L., Kraetke, R., Linders, J., Scott, M., Vighi, M., de Voogt, P. 2018. Proposed EU
688 minimum quality requirements for water reuse in agricultural irrigation and aquifer
689 recharge: SCHEER scientific advice. Current Opinion in Environmental Science & Health
690 2, 7–11.

691 Rizzo, L., Manaia, C.M., Merlin, C., Schwartz, T., Dagot, C., Ploy, M.C., Michael, I.,
692 Fatta-Kassinos, D., 2013. Urban wastewater treatment plants as hotspots for antibiotic
693 resistant bacteria and genes spread into the environment: a review. Science of the Total
694 Environment 447, 345–360.

695 Sacco, O., Vaiano, V., Rizzo, L., Sannino, D. 2018. Photocatalytic activity of a visible
696 light active structured photocatalyst developed for municipal wastewater treatment. Journal
697 of Cleaner Production 175, 38-49.

698 Trovó, A.G., Nogueira, R.F.P., Agüera, A., Sirtori, C., Fernández-Alba, A.R. 2009.
699 Photodegradation of sulfamethoxazole in various aqueous media: Persistence, toxicity and
700 photoproducts assessment. Chemosphere 77, 1292-1298.

701 USEPA. 2012. Guidelines for water reuse. (EPA/600/R-12/618) United States
702 Environmental Protection Agency, Washington, DC, USA.

703 Yuan, Q., Guo, M., Yang, J. 2015. Fate of antibiotic resistant bacteria and genes during
704 wastewater chlorination: implication for antibiotic resistance control. PloS One 10 (3),
705 e0119403.

706 Zhang, C., Brown, P.J.B., Hu, Z. 2018. Thermodynamic properties of an emerging
707 chemical disinfectant, peracetic acid. Science of the Total Environment 621, 948-959.

708 Zhang, N., Liu, G, Liu, H., Wang, Y., He, Z., Wang, G. 2011. Diclofenac
709 photodegradation under simulated sunlight: Effect of different forms of nitrogen and
710 Kinetics. Journal of Hazardous Materials 192, 411-418.

711 Figure captions

712 Figure 1. Inactivation of AR *E. coli*: control tests in dark with PAA and sunlight as
713 standalone processes. Q_{UV} values are given between brackets.

714 Figure 2. Inactivation of AR *E. coli* by sunlight/PAA in CPC: effect of initial PAA
715 concentration in GW (a) and WW (b).

716 Figure 3. Degradation of CECs: control tests with PAA and sunlight as standalone
717 processes.

718 Figure 4. Effect of sunlight/PAA process on CECs in GW: CBZ (a), DCF (b) and SMX (c).

719 Figure 5. Effect of sunlight/PAA process on CECs in WW: CBZ (a), DCF (b) and SMX
720 (c).

721 Figure 6. Inactivation of AR *E. coli* by UV-C/PAA process in GW.

722 Figure 7. Effect of UV-C/PAA process on CBZ in GW (a) and WW (b).

723 Figure 8. Effect of UV-C/PAA process on DCF in GW (a) and WW (b).

Table 1: characteristics of GW and WW samples.

	GW	WW
Parameters	**Av ± SD**	**Av ± SD**
Cl^- (mg L^{-1})	337.1 ± 76.7	341.3 ± 16.3
NO_3^- (mg L^{-1})	12.1 ± 1.2	23.4 ± 5.3
SO_4^{2-} (mg L^{-1})	200.9 ± 39.6	84.3 ± 7.7
NH_4^+ (mg L^{-1})	-	23.6 ± 24.2
Na^+ (mg L^{-1})	517.8 ± 94.1	197.5±2.8
Mg^{2+} (mg L^{-1})	67.2 ± 15.4	31.4 ± 6.9
K^+ (mg L^{-1})	8.87 ± 1.7	27.1 ± 0.8
Ca^{2+} (mg L^{-1})	71.6 ± 16.8	71.4 ± 11.8
pH	8.2 ± 0.5	7.5 ± 0.1
Conductivity (µS cm^{-1})	2396.0 ± 0.10	1921.0 ± 21.4
Turbidity (NTU)	0.6 ± 0.1	6.3 ± 4.4
TOC (mg L^{-1})	1.80 ± 1.6	24 ± 1.0
IC (mg L^{-1})	170.2 ± 9.3	38 ± 8.1
AR *E. Coli* (CFU mL^{-1})	-	1337 ± 5663

Figure1

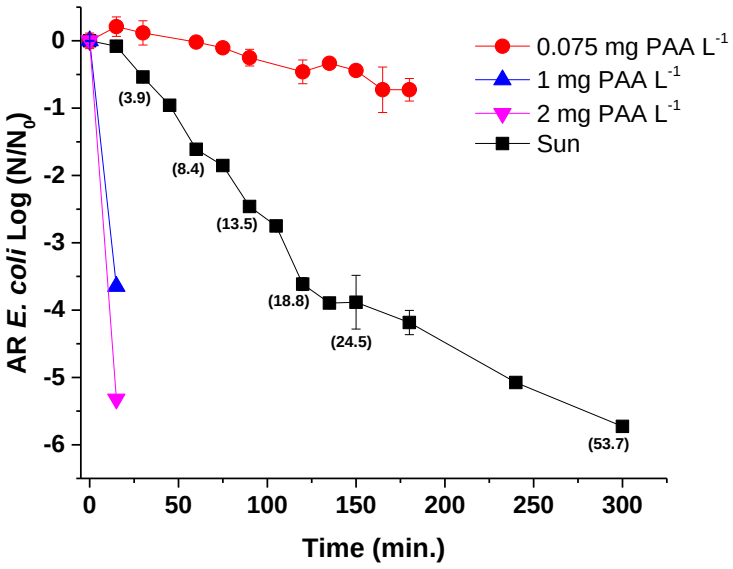

Figure 1

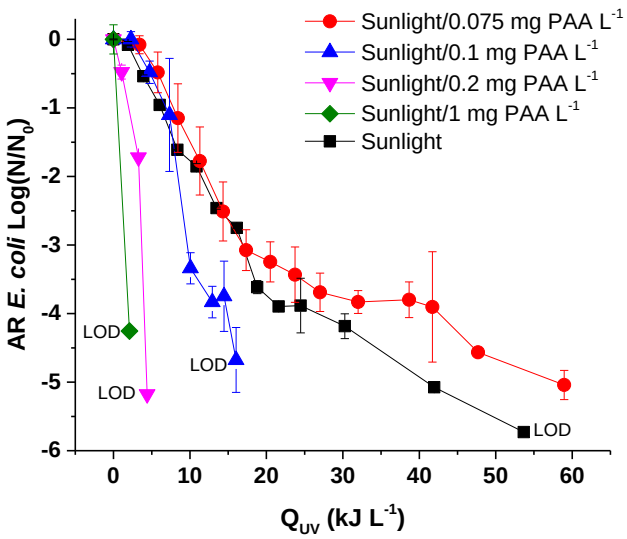
Sunlight/0.075 mg PAA L-1
Sunlight/0.1 mg PAA L-1
Sunlight/0.2 mg PAA L-1
Sunlight/1 mg PAA L-1
Sunlight
AR E. coli Log(N/N0)
QUV (kJ L-1)
LOD
LOD
LOD
LOD

a)

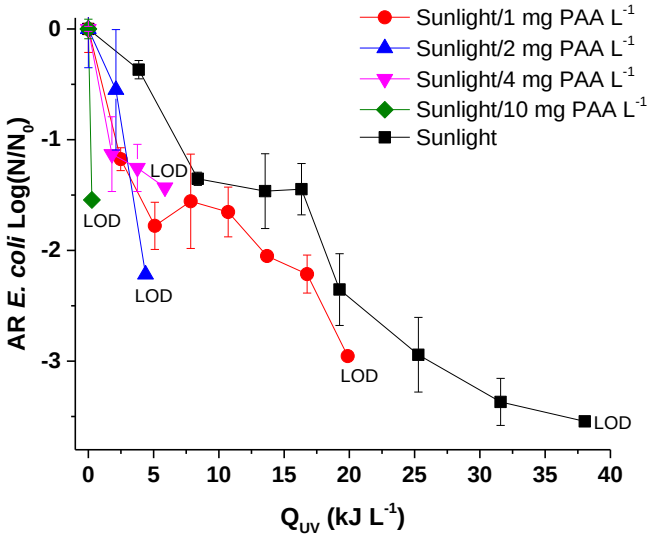
Sunlight/1 mg PAA L-1
Sunlight/2 mg PAA L-1
Sunlight/4 mg PAA L-1
Sunlight/10 mg PAA L-1
Sunlight
AR E. coli Log(N/N0)
QUV (kJ L-1)
LOD
LOD
LOD
LOD
LOD

b)

Figure 2

Figure3

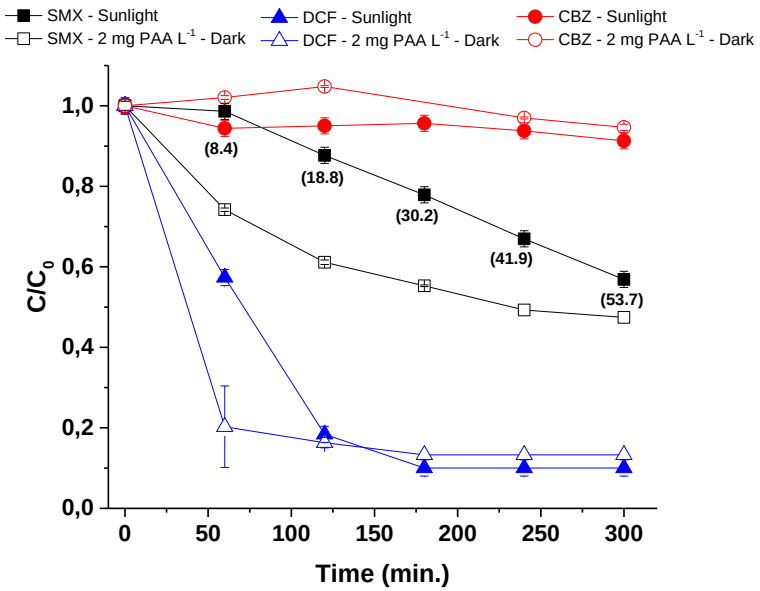

Figure 3

Figure4

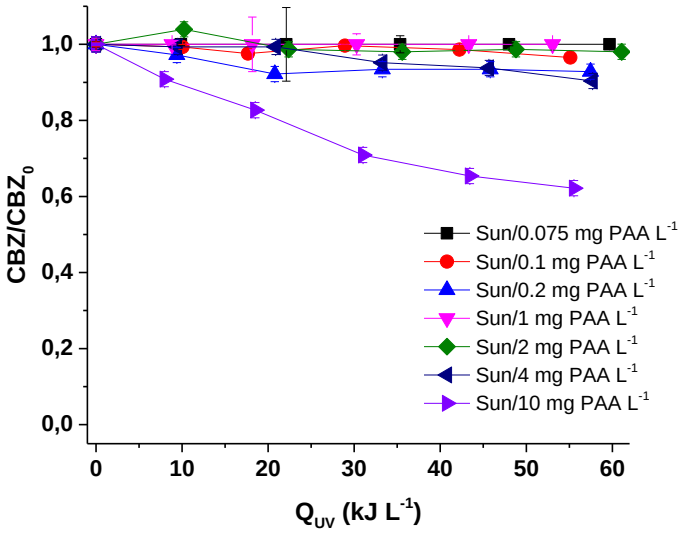

a)

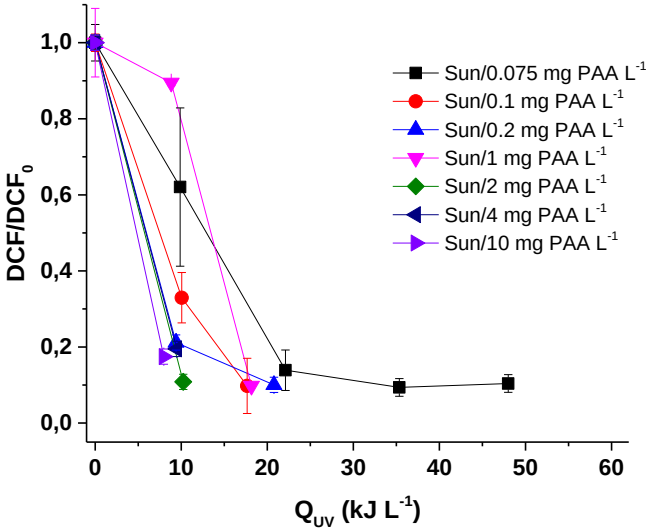

b)

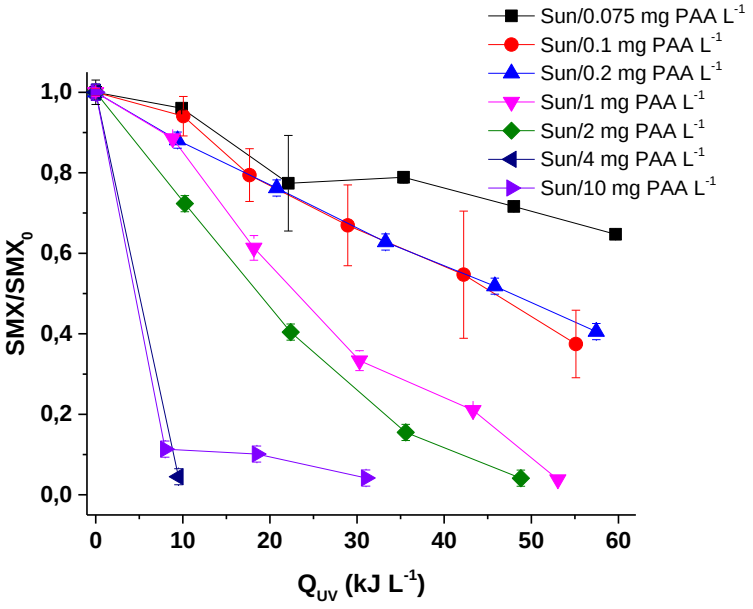

c)

Figure 4

Figure5

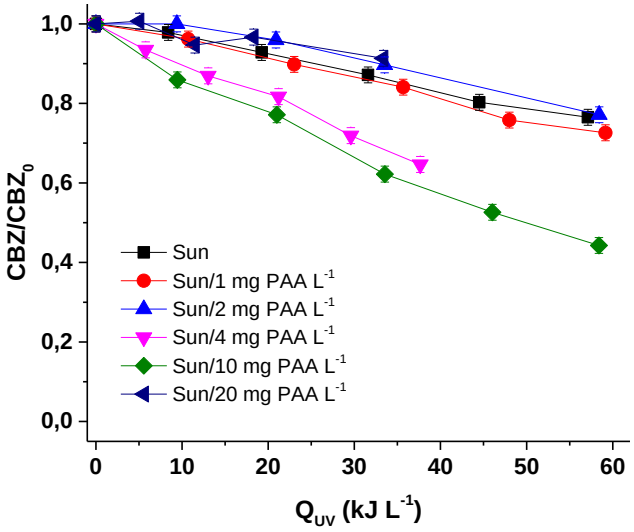

a)

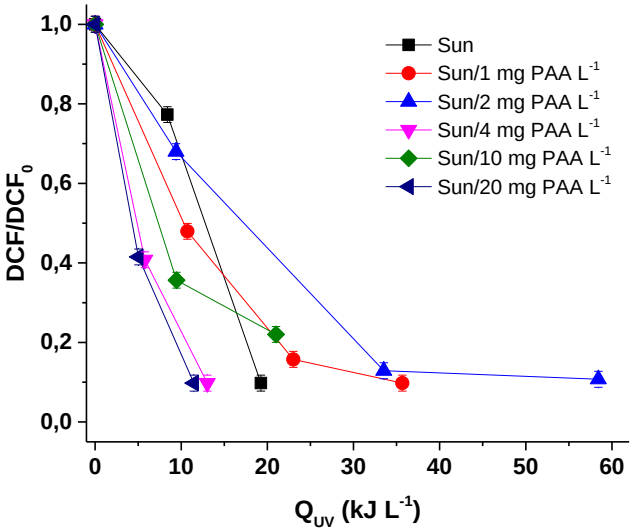

b)

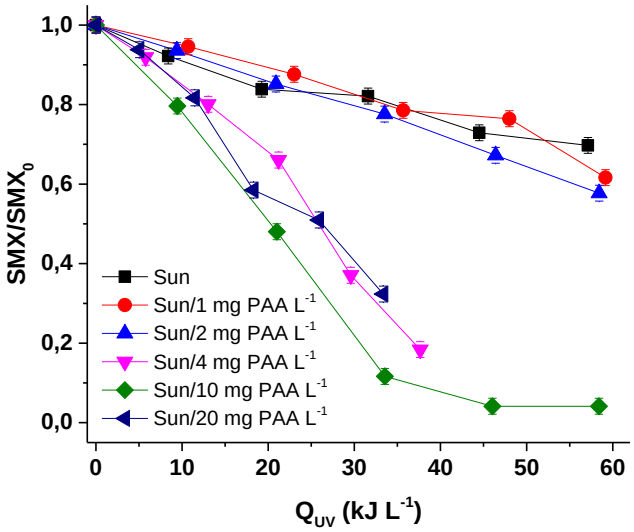

c)

Figure 5

Figure6

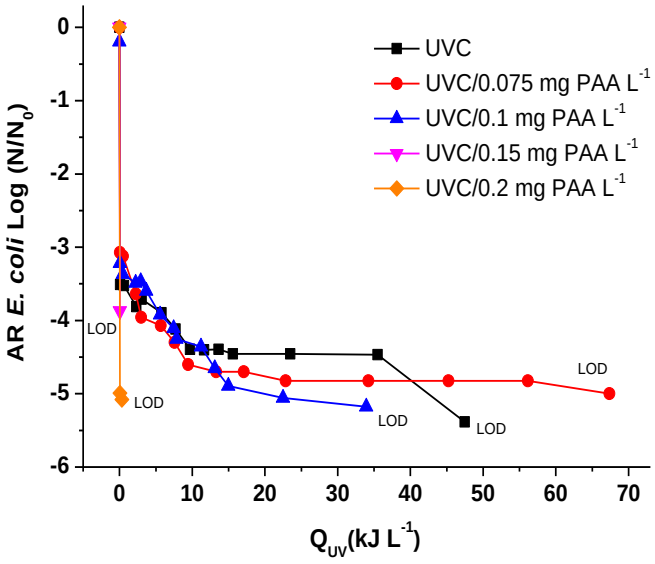

Figure 6

Figure7

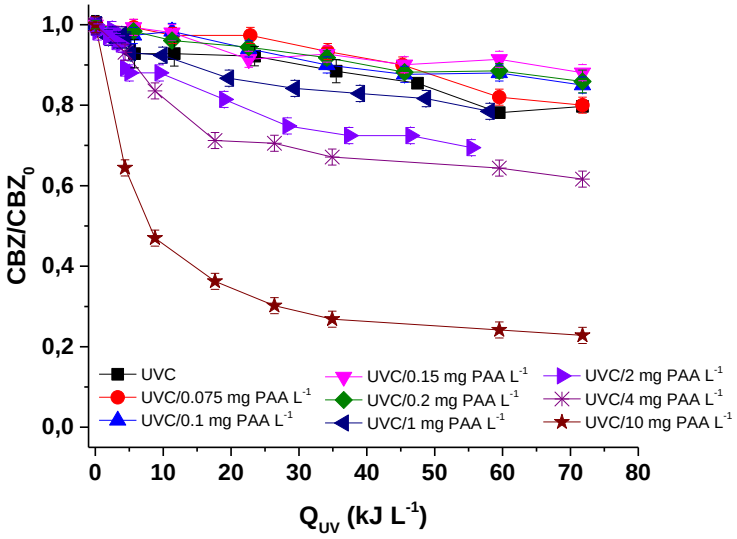

a)

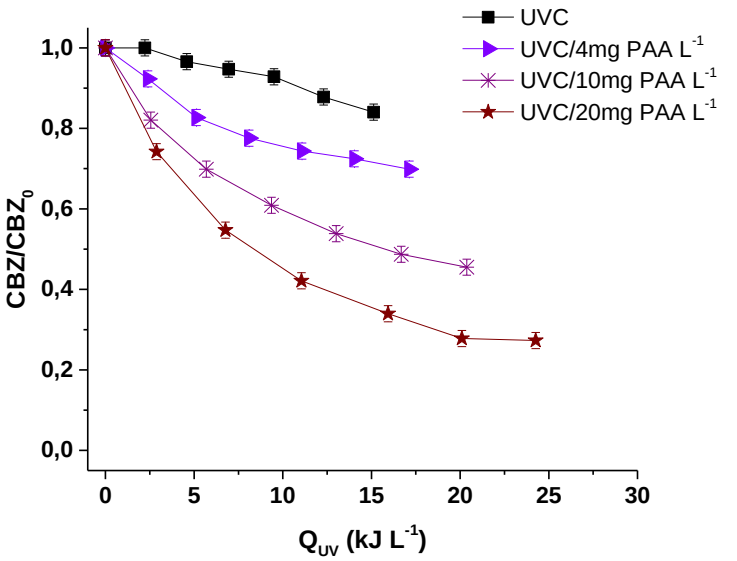

b)

Figure 7

Figure8

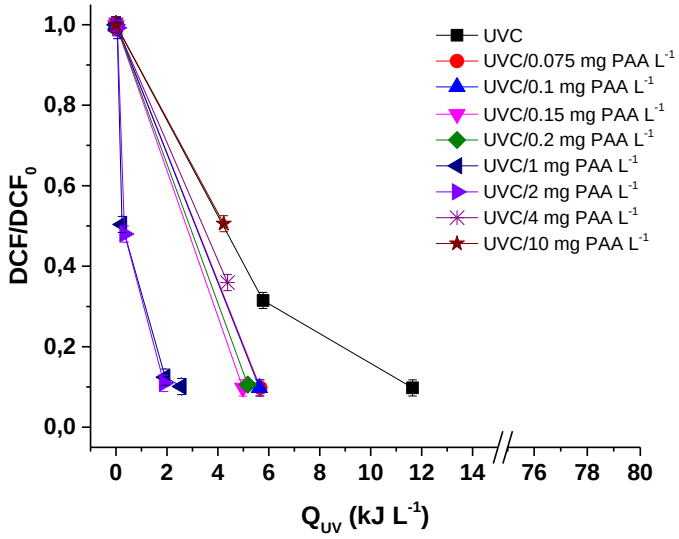

a)

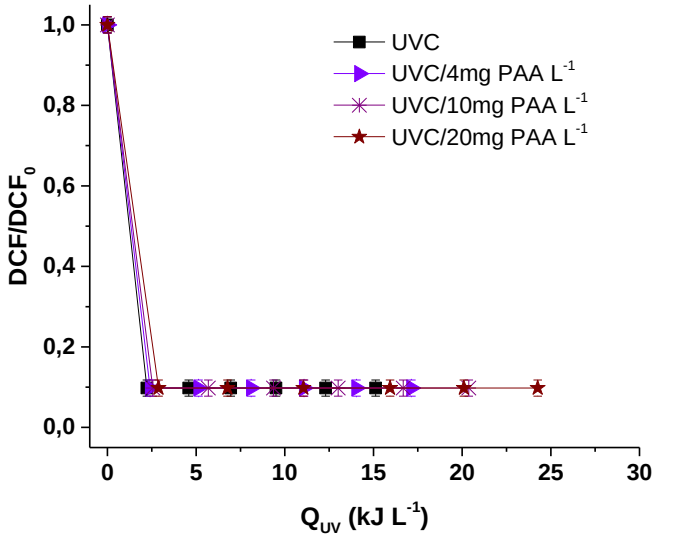

b)

Figure 8

Electronic Supplementary Material (for online publication only)

Click here to download Electronic Supplementary Material (for online publication only): Supplementary information.docx